Substrate Recognition Properties of Oligopeptidase B from *Salmonella enterica* Serovar Typhimurium

Rory E. Morty,[1]† Vilmos Fülöp,[2] and Norma W. Andrews[1]*

Section of Microbial Pathogenesis, Boyer Center for Molecular Medicine, Yale University School of Medicine, New Haven, Connecticut 06536,[1] and Department of Biological Sciences, University of Warwick, Coventry CV4 7AL, United Kingdom[2]

Oligopeptidase B (OpdB) is a serine peptidase broadly distributed among unicellular eukaryotes, gram-negative bacteria, and spirochetes which has emerged as an important virulence factor and potential therapeutic target in infectious diseases. We report here the cloning and expression of the *opdB* homologue from *Salmonella enterica* serovar Typhimurium and demonstrate that it exhibits amidolytic activity exclusively against substrates with basic residues in P_1. While similar to its eukaryotic homologues in terms of substrate specificity, *Salmonella* OpdB differs significantly in catalytic power and inhibition and activation properties. In addition to oligopeptide substrates, restricted proteolysis of histone proteins was observed, although no cleavage was seen at or near residues that had been posttranslationally modified or at defined secondary structures. This supports the idea that the catalytic site of OpdB may be accessible only to unstructured oligopeptides, similar to the closely related prolyl oligopeptidase (POP). *Salmonella* OpdB was employed as a model enzyme to define determinants of substrate specificity that distinguish OpdB from POP, which hydrolyzes substrates exclusively at proline residues. Using site-directed mutagenesis, nine acidic residues that are conserved in OpdBs but absent from POPs were converted to their corresponding residues in POP. In this manner, we identified a pair of glutamic acid residues, Glu^{576} and Glu^{578}, that define P_1 specificity and direct OpdB cleavage C terminal to basic residues. We have also identified a second pair of residues, Asp^{460} and Asp^{462}, that may be involved in defining P_2 specificity and thus direct preferential cleavage by OpdB after pairs of basic residues.

The oligopeptidase B (OpdB; EC 3.4.21.83) subfamily of serine peptidases represents one of two branches of the prolyl oligopeptidase family of serine peptidases (the S9 family, in the nomenclature of Barrett and Rawlings [2]). The archetypical member of this family, prolyl oligopeptidase (POP; EC 3.4.21.26), exclusively hydrolyzes peptide bonds C terminal to proline residues in peptides (31). It has been implicated in the pathophysiology of depression (20) and has attracted pharmaceutical attention, since POP inhibitors have shown potential in the treatment of amnesia (39) and Alzheimer's disease (36). Prolyl oligopeptidase has also served as a model for structural studies of serine oligopeptidases. A 1.4-Å crystal structure analysis of POP recently revealed that an N-terminal regulatory domain, consisting of a seven-bladed β-propeller, regulates substrate access to the C-terminal catalytic domain (7) by a gating filter mechanism (8).

In contrast to the POPs, the OpdB branch of the POP family has received much less attention. These enzymes demonstrate a trypsin-like substrate specificity, hydrolyzing peptide bonds on the C-terminal side of basic amino acid residues of low-molecular-mass (<3 kDa) peptides (17, 30, 37, 41). Of great importance for potential therapeutic applications, OpdB is only found in ancient eukaryotic unicellular organisms, in gram-negative bacteria, and in spirochetes.

Both POP (11) and OpdB (4) have been isolated from the stercorarian trypanosome *Trypanosoma cruzi*, the etiological agent of Chagas' disease, and both oligopeptidases have been implicated in the pathogenesis of this disease. In infective forms of *T. cruzi*, OpdB generates a calcium signaling factor which, via an interaction with a receptor at the mammalian cell surface (18), is responsible for the mobilization of Ca^{2+} from intracellular calcium pools (4). This Ca^{2+} signaling is a prerequisite for trypanosome invasion. Targeted deletion of the *opdB* gene in *T. cruzi* resulted in trypanosomes that were severely impaired with respect to mammalian cell Ca^{2+} signaling and invasion and were thus attenuated for virulence in a mouse model of infection (5). OpdB has also been isolated from the salivarian trypanosomes *Trypanosoma brucei* (37) and *Trypanosoma congolense* (23), and homologues have been cloned from both *T. brucei* and *Leishmania major* (25). In the case of *T. brucei* infections in mice, OpdB is released by dying parasites into the host bloodstream, where it remains stable and catalytically active. OpdB may thus contribute to the pathogenesis of African sleeping sickness through the anomalous degradation of biologically active peptides in the bloodstream of infected hosts (24). Consistent with this view, administration of irreversible OpdB inhibitors to trypanosome-infected mice significantly impaired disease progression (26, 27). Together, these reports point to important roles for this group of enzymes in microbial virulence.

The role of OpdB in the pathogenesis of several parasitic diseases and the possibility that OpdB represents a novel target for antimicrobial chemotherapy prompted an analysis of OpdB homologues from bacterial pathogens. Genes encoding OpdB

* Corresponding author. Mailing address: Section of Microbial Pathogenesis, Boyer Center for Molecular Medicine, Yale University School of Medicine, 295 Congress Ave., New Haven, CT 06536. Phone: (203) 737-2410. Fax: (203) 737-2630. E-mail: norma.andrews@yale.edu.
† Present address: Zentrum für Innere Medizin, Medizinische Klinik II, Justus Liebig Universität, D-35392 Gießen, Germany.

have been isolated from the gram-negative bacterial pathogens *Escherichia coli* (17, 32) and *Moraxella lacunata* (41) and the spirochete *Treponema denticola* (6). A preliminary analysis of OpdB function in the context of bacterial growth and protein turnover has been undertaken with *Salmonella* (13). A preliminary kinetic characterization of the *E. coli* enzyme illustrated that it cleaved substrates at the C terminus of basic residues, exhibited pronounced substrate inhibition and that the enzyme-substrate interaction was disrupted by high ionic strength, implicating ionic interactions in substrate binding (16, 29, 32). However, OpdB homologues from prokaryotes have not been extensively characterized, particularly with respect to substrate recognition properties and roles in bacterial virulence. In this report, we have addressed the former issue, showing that while catalytically similar to its eukaryotic homologues in terms of substrate affinity, OpdB from *Salmonella* exhibits a diminished catalytic capacity and differs in inhibition and activation properties. We go on to demonstrate that OpdB, in addition to low-molecular-mass peptides, can cleave in a restricted fashion several basic proteins, including human histones H1, H2A, H3, and H4. We have also used *Salmonella* OpdB as a model enzyme to define structural elements that are responsible for differences in the substrate recognition properties of OpdB and the closely related POP. These elements include two pairs of conserved acidic residues that are likely to direct P_1 and P_2 substrate specificity (using the nomenclature of Schechter and Berger [35]) for this subfamily of enzymes.

MATERIALS AND METHODS

Bacterial strains and growth conditions. *Salmonella enterica* serovar Typhimurium virulent, wild-type strain SL1344 (14) was obtained from Jorge E. Galán (Yale University School of Medicine, New Haven, Conn.) and propogated in Luria-Burtani (LB) broth (1% [mass/vol] NaCl, 1% [mass/vol] tryptone, 0.5% [mass/vol] yeast extract) or on LB agar (LB broth containing 1.5% [mass/vol] agar), supplemented with streptomycin (50 μg · ml^{-1}). *E. coli* cloning (DH5α, Gibco; TOP10F', Invitrogen) and expression [BL21(λDE3); Novagen] strains were cultured in LB media containing ampicillin (100 μg · ml^{-1}) or kanamycin (30 μg · ml^{-1}) as appropriate.

Isolation of the *Salmonella opdB* gene. Using the *E. coli opdB* sequence (17), forward (5'-CCA GAA AGA ACA ATA ACA TGC TAC CAA AAG CC-3') and reverse (5'-GTA GAT CAG TTT ATC TTG CGA TG-3') primers were synthesized complementary to the *E. coli* sequence and used to generate a 668-bp probe using *Salmonella* genomic DNA, isolated as described in reference 38, as a template. The PCR product was cloned into pCR2.1 (Invitrogen) to create pNA102, from which the *opdB* fragment could be excised using the flanking *Eco*RI sites. Radiolabeled DNA probes were prepared using the purified DNA fragment (25 ng) as a template for random prime labeling (Rediprime; Amersham) with 50 μCi of [α-^{32}P]dCTP. *Salmonella* genomic DNA was subjected to single and double digests with various restriction endonucleases. Digested DNA was resolved on a 0.7% (mass/vol) agarose gel, transferred to a Hybond N+ nylon membrane, and probed with the [α-^{32}P]dCTP-labeled probes as described previously (4). Probes were hybridized with a ±3.5-kb fragment from a *Sal*I/*Hin*dIII double digest of *Salmonella* DNA (not shown). Genomic DNA was double digested with *Sal*I and *Hin*dIII and resolved on a 0.7% (mass/vol) low-melting-point agarose gel, and DNA was extracted from a gel slice containing fragments in the 3- to 4-kb size range. Fragments were cloned into the *Sal*I and *Hin*dIII sites of pBlueScript II KS(+) (Stratagene) and transformed into *E. coli* TOP10F'. Colonies could not be screened by hybridization due to annealing of the probe with the genomic DNA-encoded *E. coli opdB* gene. Colonies were pooled into batches of 50, from which plasmid DNA was screened by PCR. Colonies from PCR-positive batches were screened individually, and a single PCR-positive clone containing a ±3.5-kb fragment (pNA104) was sequenced in both directions from the T3 and T7 pBlueScript II K(+) promoters using T3 (5'-AAT TAA CCC TCA CTA AAG GG-3') and T7 (5'-GTA ATA CGA CTC ACT ATA GGG C-3') sequencing primers. This construct contained the full-length *Salmonella opdB* gene. Nucleotide sequencing was undertaken by the W. M. Keck Foundation Biotechnology Resource Laboratory at Yale University.

Expression of recombinant OpdB. The *Salmonella opdB* gene was amplified by PCR from pNA104 with *Pfu*Turbo polymerase (Stratagene) using forward (5'-GA AAA **CTC GAG** <u>ATG</u>TTG CCA AAA GCC AAT CGA ATT CCC-3') and reverse (5'-TAC GCT **CTC GAG** CTA TGC GCT ATG TAA GGT TCC CTG CGC-3') primers (with internal *Xho*I sites in boldface type; the initiation codon of the forward primer is underlined). The PCR product was cloned into the *Sma*I site of pBlueScript II KS(+) to create pNA110, and the 2.1-kb *Xho*I-*Xho*I fragment was excised from pNA110 and subcloned into the pET19b expression vector (Novagen) to create pNA111. Sequencing from the pET19b T7 promoter using the T7 forward sequencing primer (5'-TAA TAC GAC TCA CTA TAG G-3') demonstrated that fragment was correctly orientated and the ATG start codon was in frame.

For expression, pNA111 was transformed into *E. coli* BL21(λDE3). N-terminal polyhistidine-tagged fusion proteins were expressed by induction of a log-phase culture ($A_{600} \approx 0.6$) with 1 mM isopropyl-β-D-thiogalactopyranoside (IPTG) for 16 h at 27°C with vigorous (270 rpm) shaking in the presence of ampicillin (100 μg · ml^{-1}). Bacteria from a 500-ml culture were harvested by centrifugation (7,000 $\times$ g, 10 min, 4°C); resuspended in 20 mM Tris-HCl, 5 mM imidazole, and 500 mM NaCl (pH 7.9) (25 ml, 4°C); and sonicated on ice with a Branson 250 sonicator (duty cycle = 80%, output control = 8; four cycles were carried out for 2 min each time). Bacterial lysates were clarified by centrifugation (15,000 $\times$ g, 15 min, 4°C) and passage through a 0.45-μm syringe filter unit, prior to peptidase purification on Ni^{2+}-agarose (Novagen) according to the manufacturer's specifications. In some instances, the polyhistidine tag was removed with an Enterokinase Cleavage Capture kit (Novagen).

Nucleotide and protein sequence alignments. An unrooted dendrogram was prepared, comparing full-length amino acid sequences of 18 members of the POP family with the CLUSTAL W software from the MEGALIGN program (DNASTAR, Madison, Wis.), with a PAM250 weight table set with the following parameters: ktuple = 1, gap penalty = 3, and gap window = 5 (1).

Site-directed mutagenesis. The pNA111 expression construct was employed as a template for the generation of site-directed OpdB mutants. Site-directed mutagenesis was performed using the PCR-based Quickchange system (Stratagene). Mutagenic oligonucleotide primers were synthesized containing single- or multiple-base-pair changes with at least 15 bp of flanking sequence on either side of the base pair change. Base pair changes were confirmed by DNA sequencing from either the pET19b T7 terminator with a T7 terminator primer (5'-GCT AGT TAT TGC TCA GCG G-3') or from a reverse primer complementary to bp 1648 to 1664 of the *opdB* gene (5'-CCA TAA CAC AAG CGA CGG-3').

Kinetic analysis of recombinant OpdB. Substrate specificity of OpdB was determined using fluorogenic substrates, by preincubation of OpdB (20 to 60 fmol of active enzyme, 37°C, 5 min) in 50 mM Tris-HCl, pH 8, followed by addition of substrate. The initial steady-state velocity (v_0) was determined by continuous assay for a range of substrate concentrations (50 nM to 100 μM). K_m and V_{max} values were determined by hyperbolic regression of the kinetic data using the software package Hyper 1.01 (obtained from J. S. Easterby, University of Liverpool, Liverpool, United Kingdom). The k_{cat} was determined from the expression $k_{cat} = V_{max}/[E]_0$, where $[E]_0$ represents the active enzyme concentration, determined by active-site titration with 4-methylumbelliferyl-*p*-guanidinobenzoate as described previously (25). Fluorogenic leaving groups were detected with a Hitachi F-2000 spectrofluorimeter at excitation and emission wavelengths of 370 and 460 nm, respectively, for 7-amino-4-methylcoumarin (AMC) (25) and 337 and 420 nm for β-naphthylamide (βNA) (9). Hydrolysis of *para*-nitroanilide (pNA) substrates was monitored spectrophotometrically at 405 nm with a Pharmacia Biotech Ultraspec 2000 spectrophotometer (29).

The effect of reducing agents on OpdB activity was investigated by preincubating OpdB in assay buffer containing L-cysteine, β-mercaptoethanol, dithiothreitol, or reduced glutathione (1 to 25 mM, 37°C, 5 min) prior to the addition of Carbobenzyloxy (Cbz)-Arg-Arg-AMC (to 5 μM).

For reversible competitive inhibitors, the K_i value was determined as described in reference 33. The enzyme-catalyzed hydrolysis of Cbz-Arg-Arg-AMC was monitored continuously to establish an uninhibited rate of substrate hydrolysis (v_0), after which a 20-fold molar excess of inhibitor over enzyme was added (in less than 5% of the total assay volume), and the new steady-state velocity in the presence of the inhibitor (v_i) determined. The apparent inhibition constant in the presence of substrate [$K_{i(app)}$] was given by the expression $v_0/v_i = 1 + [I]/K_{i(app)}$. The true K_i was calculated for competitive inhibitors (I), catering for the presence of substrate, from the relationship $K_i = K_{i(app)}/1 + [S]/K_m$, where [S] indicates substrate concentration.

The effects of irreversible peptidase inhibitors were investigated as described in reference 33 by adding an aliquot of inhibitor (10 μl) to a buffered enzyme
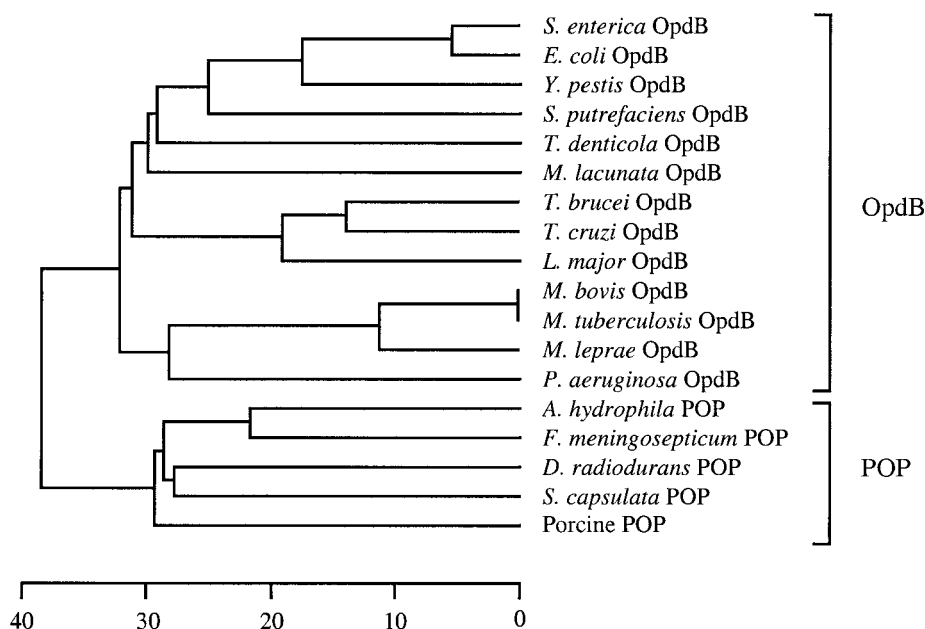
FIG. 1. Phylogenetic relationship of members of the POP family of serine peptidases. An unrooted dendrogram was prepared by comparing the full-length amino acid sequences of 18 members of the POP family using the CLUSTAL W alignment software of the MEGALIGN program (DNASTAR) with a PAM250 weight table set with the following parameters: ktuple = 1, gap penalty = 3, gap window = 5. The scale at the bottom measures the distance between sequences. The units indicate the number of substitution events (as a percentage). Sequences were obtained from the GenBank/EBI database under the following accession numbers: D10976 (*E. coli* OpdB), AF078916 (*T. brucei* OpdB), U69897 (*T. cruzi* OpdB), AF109875 (*L. major* OpdB), D38405 (*M. lacunata* OpdB), Z80226 (*Mycobacterium tuberculosis* OpdB), Z95151 (*Mycobacterium leprae* OpdB), AAK39550 (*T. denticola* OpdB), D14005 (*Aeromonas hydrophila* POP), D10980 (*Flavobacterium meningosepticum* POP), U08343 (*Deinococcus radiodurans* POP), AB010298 (*Sphingomonas capsulata* POP) and M64227 (porcine brain POP). The OpdB sequences for *Y. pestis* and *Mycobacterium bovis* were extracted from their partially sequenced genomes at the Sequencing Group at the Sanger Centre (available at www.sanger.ac.uk). The OpdB sequences from *S. putrefaciens* and *Vibrio cholerae* were extracted from their partially sequenced genomes at The Institute for Genome Research (available at www.tigr.org). The *Pseudomonas* OpdB sequence was extracted from the partially sequenced *Pseudomonas* genome at the *Pseudomonas* Genome Project (available at www.pseudomonas.com).

solution (140 µl, containing 90 to 150 ng of OpdB in 50 mM Tris-HCl [pH 8.0], 37°C) to initiate the inactivation. Aliquots were removed at timed intervals and residual activity (v_t) was determined against Cbz-Arg-Arg-AMC as described above. Pseudo-first-order inhibition rate constants (k_{obs}) were obtained from plots of ln v_t/v_0 versus time, where v_0 represents the activity prior to addition of inhibitor. Second-order inhibition rate constants (k_{ass}) were obtained from the expression $k_{ass} = k_{obs}/[I]$, where [I] represents inhibitor concentration.

Histone degradation by OpdB. Human histones H1, H2A, H3, and H4 (Roche Molecular Biochemicals) were prepared as aqueous 1-mg · ml⁻¹ solutions. Reaction mixtures, composed of histone (10 µg) and OpdB (0.1 to 10 µg; giving enzyme/substrate ratios of 1:100, 1:10, and 1:1) in 50 mM Tris-HCl, pH 8, were incubated at 37°C. Samples, incubated for 20 min, 1 h, 4 h, and 12 h, were resolved by reducing Tris-Tricine sodium dodecyl sulfate-polyacrylamide gel electrophoresis (SDS-PAGE) on 16% polyacrylamide gels containing 6 M urea (34), and protein was detected with Coomassie blue. For N-terminal analysis, proteins were electroblotted onto polyvinylene difluoride membranes as described in reference 21 and N-terminal analysis was undertaken by the W. M. Keck Foundation Biotechnology Resource Laboratory at Yale University.

Fluorescence measurements. Steady-state fluorescence intensities and emission spectra were recorded with a Hitachi F-2000 spectrofluorimeter with excitation and emission slit widths of 2 nm and an excitation wavelength of 278 nm. To monitor the unfolding transition of OpdB and its site-mutated variants as a function of guanidine hydrochloride (GuHCl) concentration, aliquots of GuHCl (50 to 1,000 µl) were added from an 8 M stock to the sample (final concentration, 25 µg · ml⁻¹ in 50 mM Tris-HCl, pH 8; final volume, 2 ml). Samples were equilibrated at 25°C before the emission spectrum was recorded.

Nucleotide sequence accession number. The nucleotide sequence of *S. enterica* serovar Typhimurium *opdB* is available under GenBank/EBI database accession number AF237705.

RESULTS

Analysis and expression of the *Salmonella opdB* gene. The *opdB* gene isolated from *S. enterica* serovar Typhimurium strain SL1344 contained an open reading frame of 2,052 bp, encoding a polypeptide of 684 amino acids with a predicted molecular mass of 78.969 kDa. The polypeptide contained a POP family consensus sequence (GXSXGGZZ, where X = any residue and Z = a hydrophobic residue [3]) at residues 530 to 537, which harbors the active-site serine residue. The *opdB* gene from this highly virulent *Salmonella* strain (SL1344) contained a single thymine→cytosine base pair change (at nucleotide 182) when compared with the *opdB* gene found in the genome sequence of nonvirulent *S. enterica* serovar Typhimurium strain LT2 (22), resulting in a Thr[61]→Ile[61] replacement. The *Salmonella opdB* gene exhibited 75% identity with its *E. coli* homologue (17), and their encoded proteins share 89% identity. *Salmonella* OpdB retained a high degree of identity to OpdB from several other members of the gamma subdivision of the *Proteobacteria* (Fig. 1), including *Yersinia pestis* (63%) and *Schewanella putrefaciens* (44%). Interestingly, *Salmonella* OpdB exhibited higher identity to the deduced amino acid sequence of several eukaryotic *opdB* homologues, including those from the eukaryotes *T. brucei* (33%) and *L. major*

TABLE 1. Substrate specificity of *Salmonella* OpdB

Substrate[a,b]	Kinetics		
	K_m (μM)	k_{cat} (s^{-1})	k_{cat}/K_m (s^{-1} μM^{-1})
Cbz-Arg-Arg-AMC	0.8	29	36
Boc-Leu-Lys-Arg-AMC	1.0	28	28
Boc-Leu-Arg-Arg-AMC	1.1	26	24
Boc-Gly-Arg-Arg-AMC	1.9	23	12
Cbz-Gly-Gly-Arg-AMC	2.3	25	11
Boc-Gly-Lys-Arg-AMC	1.9	20	11
Cbz-Phe-Arg-AMC	2.1	21	10
Boc-Leu-Thr-Arg-AMC	2.2	18	8
Boc-Leu-Gly-Arg-AMC	2.6	20	8
Boc-Leu-Gly-Lys-AMC	2.4	16	7
Boc-Gln-Gly-Arg-AMC	2.8	17	6
Cbz-Val-Arg-AMC	2.6	15	6
Cbz-Gly-Arg-AMC	3.4	15	4
Tos-Gly-Pro-Lys-AMC	8.1	18	2
Cbz-Arg-AMC	4.4	9	2
Tos-Gly-Pro-Arg-AMC	9.9	13	1
Cbz-Lys-AMC	5.4	7	1

[a] No activity was observed against H-Arg-AMC, H-Leu-AMC, H-Lys-AMC, Cbz-Leu-Leu-Glu-βNA, Cbz-Gly-Gly-Leu-pNA, Cbz-Ala-Ala-Phe-AMC, Suc-Ile-Ala-AMC, Suc-Gly-Pro-AMC, Ac-Tyr-Val-Ala-Asp-pNA, and Suc-Ala-Ala-Pro-Phe-AMC. Standard errors of K_m and k_{cat} values were within 7% of their respective means.
[b] Kinetic constants for *Salmonella* OpdB from which the polyhistidine affinity tag had been removed were as follows: for Cbz-Arg-Arg-AMC, $K_m = 0.88$ μM, $k_{cat} = 34$ s^{-1}, and $k_{cat}/K_m = 38.64$ s^{-1} μM^{-1}; for Cbz-Arg-AMC, $K_m = 5.1$ μM, $k_{cat} = 10$ s^{-1}, and $k_{cat}/K_m = 1.96$ s^{-1} μM^{-1}.

TABLE 2. Inhibition of *Salmonella* OpdB

Inhibitor[a]	Inhibition constant	
	K_i (μM)	k_{ass} (M^{-1} s^{-1})
Reversible		
para-Aminobenzamidine	117.1	
Benzamidine	186.7	
Leupeptin	0.4	
Antipain	0.0081	
Irreversible inhibitors		
3,4-Dichloroisocoumarin		129.0 ± 12
4-(2-Aminoethyl)benzenesulfonyl fluoride		31.1 ± 8
Phenylmethane sulfonylfluoride		0.2 ± 0.04

[a] No inhibition of activity of the wild-type enzyme was observed with iodoacetamide (1 mM), iodoacetate (1 mM), *N*-ethylmaleimide (1 mM), EDTA (1 mM), EGTA (1 mM), bestatin (10 μM), amastatin (10 μM), arphamenine A (10 μM), elastinal (10 μM), dynorphin A (10 μM), or dynorphin B (10 μM). The standard error of the K_i values was within 5% of the mean.

(33%), than it did to OpdB from some prokaryotes, for example, three *Mycobacterium* species (31 to 32%). The wild-type *opdB* gene and its site-mutated variants were expressed in *E. coli* as soluble, catalytically active polyhistidine affinity-tagged enzymes with protein yields of between 10 to 15 mg per liter of bacterial culture.

Amidolytic activity of recombinant *Salmonella* OpdB. Recombinant OpdB exhibited hydrolytic activity against several fluorogenic substrates (Table 1). The best substrate for the peptidase was Cbz-Arg-Arg-AMC with a $k_{cat}/K_m = 36$ s^{-1} μM^{-1}, comparing well with the 63 s^{-1} μM^{-1} reported for the *E. coli* homologue (30). Removal of the N-terminal polyhistidine affinity tag did not alter the kinetic profile (Table 1), illustrating that the tag did not interfere with catalysis. This is consistent with our previous report that a polyhistidine affinity-tagged recombinant OpdB from *T. brucei* behaved identically to the native enzyme isolated directly from trypanosomes (25). OpdB only hydrolyzed peptide substrates with basic amino acid residues (arginine or lysine) in the P_1 position (using the nomenclature of Schechter and Berger [35]; Table 1), although no activity was observed against the aminopeptidase substrates H-Arg-AMC and H-Lys-AMC. Hydrolytic activity was observed when the N terminus of H-Arg-AMC was blocked with a Cbz group (i.e., Cbz-Arg-AMC; $k_{cat}/K_m = 2$ s^{-1} μM^{-1}). Further lengthening of the peptide (Cbz-Arg-Arg-AMC; $k_{cat}/K_m = 36$ s^{-1} μM^{-1}) considerably (18-fold) improved activity, suggesting that substrate hydrolysis is more efficient when multiple substrate-binding sites are occupied. Arginine appeared to be the preferred P_1 residue, since replacement of Arg in Cbz-Arg-AMC with Lys was accompanied by a 50% reduction in k_{cat}/K_m (Table 1). Many different residues could be accommodated in P_2, including aromatic (Phe), hydrophobic (Val), hydrophilic (Thr), small uncharged (Gly) residues and proline. However, basic residues (Arg and Lys) were also favored in P_2. Both arginine and lysine appeared equally acceptable in P_2 (since replacement of the P_2-Arg with Lys in Boc-Leu-**Arg**-Arg-AMC and Boc-Gly-**Arg**-Arg-AMC (the replacement site is shown in boldface) did not appreciably [9%] alter the K_m).

In contrast to its eukaryotic homologues, *Salmonella* OpdB did not demonstrate reductive activation, since preincubation with L-cysteine, β-mercaptoethanol, dithiothreitol, and reduced glutathione had no affect on activity against Cbz-Arg-Arg-AMC (not shown). Similarly, OpdB activity was not influenced by thiol-alkylating agents, including iodoacetamide, iodoacetate and *N*-ethylmaleimide (not shown), although these compounds are potent inhibitors of eukaryotic OpdB. *Salmonella* OpdB was rapidly inactivated by irreversible serine peptidase inhibitors, 4-(2-aminoethyl)benzenesulfonyl fluoride, 2,3-dichloroisocoumarin, and phenylmethane sulfonylfluoride at rates comparable to those for eukaryotic OpdB (25). *Salmonella* OpdB was potently inhibited by the tripeptide aldehydes antipain and leupeptin (Table 2) although the arginine analogues benzamidine and *para*-aminobenzamidine were comparatively poor inhibitors (Table 2), supporting our earlier suggestion that substrate (or inhibitor) binding is more effective when multiple substrate-binding sites are occupied.

Histone hydrolysis by recombinant *Salmonella* OpdB. Several histone degradation products were observed upon coincubation with recombinant polyhistidine affinity-tagged OpdB at an enzyme/substrate ratio of 1:10 for 4 h (Fig. 2A). Identical data were obtained using recombinant OpdB from which the polyhistidine affinity tag had been removed (data not shown). Proteolysis was limited, since identical digestion patterns were observed with three different enzyme/substrate ratios (including 1:100, 1:10, 1:1), and in the case of H2A and H4, a enzyme/substrate ratio of 10:1 was also attempted (data not shown). Upon 4 h of coincubation with OpdB, histones H2A and H4 each yielded two major degradation products (enzyme/substrate ratio, 1:10) (Fig. 2A). These degradation products appear to be generated simultaneously, since they appear at similar relative intensities at 1, 4, and 12 h and are not evident at
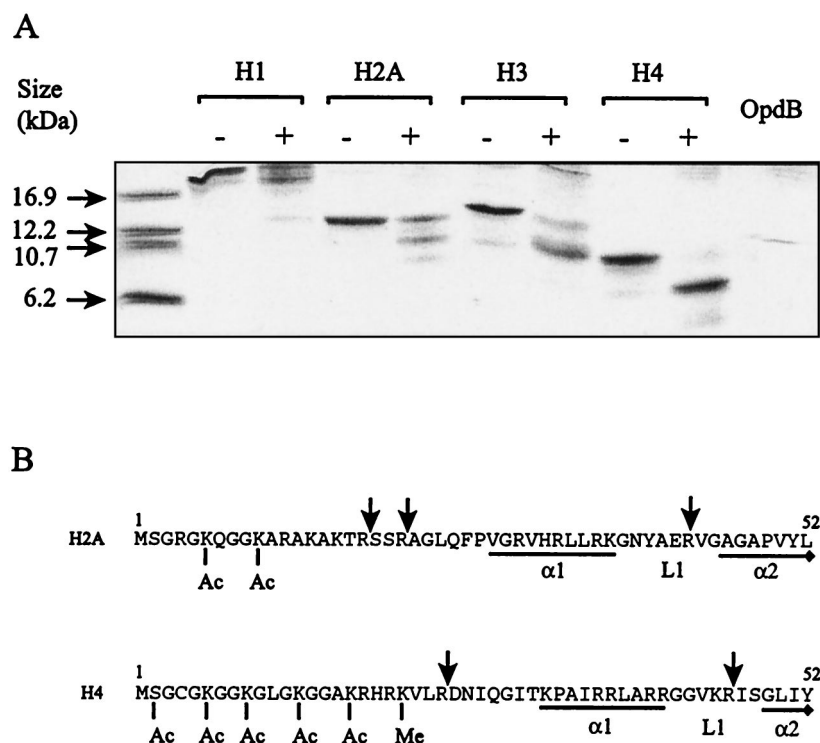
FIG. 2. Degradation of histone proteins by OpdB. Reactions consisted of histone proteins (10 μg) incubated alone (indicated by −) or together with recombinant polyhistidine affinity-tagged OpdB (1 μg; indicated by +) in 50 mM Tris-HCl, pH 8, for 4 h. As a control, recombinant polyhistidine affinity-tagged OpdB (1 μg) was incubated without histone proteins (OpdB) under the same conditions. (A) Samples were resolved by reducing Tris-Tricine SDS-PAGE on 16% polyacrylamide gels containing 6 M urea. (B) Selected degradation products were blotted onto polyvinylidene difluoride membranes, and cleavage points were identified by N-terminal amino acid sequence analysis. Cleavage points in the H2A and H4 N-terminal regions are indicated by an arrow (↓). Residues that are acetylated (Ac) and methylated (Me) in vivo are indicated. The first two α-helices of the core histone domains and their connecting random loops are indicated by α1, α2, and L1, respectively. Residues forming α-helices are underlined. Residue numbering is shown above the first and last residues in each sequence.

20 min (not shown). Thus, cleavage at the N-terminal proximal site and the N-terminal distal site probably takes place independently, not sequentially. Several cleavage points were identified in H2A and H4 by N-terminal analysis of the degradation products. Hydrolysis was always observed C terminal to an Arg residue and occurred only after residues that were not post-translationally modified, or locked into defined secondary structures such as α-helices (Fig. 2B). The major OpdB cleavage sites in the H2A molecule were identified by N-terminal analysis as Arg^{18} ↓ Ser^{19}, Arg^{21} ↓ Ala^{22} and Arg^{43} ↓ Val^{44}, and in the H4 molecule as Arg^{24} ↓ Asp^{25} and Arg^{46} ↓ Ile^{47}. Histone hydrolysis by OpdB was abrogated in the presence of anti-OpdB antibodies (not shown). Since anti-OpdB antibodies are potent and selective inhibitors of OpdB (24), we are confident that it was OpdB, and not residual contaminating *E. coli* peptidases, that is responsible for the observed hydrolysis of histone proteins.

Alignment of catalytic domains in POP and OpdB. Amino acid sequence alignment of the C-terminal catalytic domain of five OpdB and three POP sequences (Fig. 3) revealed several stretches of sequence or individual residues that were conserved within respective branches of the phylogenetic tree (Fig. 1) but were consistently different between the two branches. We proposed that residues contained within these differentially conserved stretches of sequence were likely to be respon-

sible for substrate specificity. In particular, aspartic or glutamic acid residues conserved in the OpdB group of enzymes were of interest, since they would facilitate electrostatic interaction with the basic amino acid side chains of arginine and lysine residues in substrates. Nine such residues, Asp^{460}, Asp^{462}, Glu^{494}, Asp^{567}, Glu^{576}, Glu^{578}, Asp^{599}, Glu^{624}, and Asp^{638}, were targeted for mutagenesis studies. Site-mutated variants were expressed equally well as the wild-type enzyme in *E. coli* and, after two passages over Ni^{2+}-agarose, were almost 100% pure, as judged by a Coomassie blue stained SDS-PAGE gel (not shown).

Fluorescence emission spectra of recombinant *S. enterica* serovar Typhimurium OpdB. Emission spectra for all the native forms of all OpdB variants peaked at 336 nm (λ_{max}) and showed a bathochromic (red) shift in λ_{max} to 366 nm in the presence of 4 M GuHCl. Fluorescence emission spectra of native and GuHCl-denatured wild-type OpdB and the D460T-D462N and E576A-E578A site-mutated OpdB variants are illustrated in Fig. 4A. All mutants also exhibited identical unfolding transitions in the presence of increasing GuHCl concentrations (Fig. 4B). In the interests of clarity, only spectra for the wild-type, D460T-D462N, and E576A-E578A site-mutated OpdB variants are illustrated. The remaining nine site-mutated OpdB variants exhibited superimposable native and GuHCl-denatured emission spectra. These data strongly suggest that

FIG. 3. Multiple sequence alignment of the amino acid sequences of the catalytic domains of OpdB from representatives of the OpdB and POP branches of the prolyl endopeptidase family of serine peptidases. Sources of sequences are given in the legend to Fig. 1. The active-site serine, histidine, and aspartic acid residues that constitute the catalytic triad are indicated by asterisks. Residues that were mutated in this study are grouped in boxes.

differences in the observed kinetic properties of the wild-type and active-site mutated variants of OpdB are not due to the disruption of the structural integrity of the enzyme (although it remains possible that very subtle structural changes were not detected in the emission spectra).

Effect of point mutations on P₁ substrate specificity. The substrate Cbz-Arg-AMC was employed to monitor changes in P₁ substrate specificity of site-mutated OpdB variants. Only two mutations, those in Glu^{576} and Glu^{578}, resulted in significant changes in the hydrolysis of Cbz-Arg-AMC by OpdB (Table 3). Replacement of Glu^{576} with alanine (E576A) caused a 7.6-fold elevation in the K_m and a 4.5-fold reduction in the k_{cat}, in comparison to the wild-type enzyme (Table 3). Similarly, although less dramatic, replacement of Glu^{578} with alanine (E578A) resulted in a 3.7-fold elevation in K_m and a 2.3-fold reduction in k_{cat}. Simultaneous replacement of both Glu^{576} and Glu^{578} with tryptophan and threonine, respectively, (E576W:E578T), or with alanines (E576A:E578A) or arginines (E576R:E578R), abolished OpdB activity against Cbz-Arg-AMC (Table 3).

Effect of point mutations on P₂ substrate specificity. The substrates Cbz-Arg-Arg-AMC and Cbz-Phe-Arg-AMC were employed to monitor changes in P₂ substrate specificity of site-mutated OpdB variants. Only two mutations, those in Asp^{460} and Asp^{462}, altered the hydrolytic activity of OpdB against Cbz-Arg-Arg-AMC (Table 4) apart from Glu^{576} and

Glu^{578}. Mutation of Asp^{460} to threonine (D460T) caused a 2.6-fold elevation in K_m for Cbz-Arg-Arg-AMC hydrolysis and a 24% reduction in k_{cat}. Similarly, replacement of Asp^{462} with Asn (D462N) caused a threefold elevation in K_m and a 21% reduction in k_{cat} for Cbz-Arg-Arg-AMC hydrolysis. Simultaneous replacement of Asp^{460} and Asp^{462} with threonine and asparagine, respectively (D460T-D462N) had a more pronounced affect than the single mutations, yielding an OpdB variant with a 3.6-fold increase in K_m and a 38% reduction in k_{cat} for Cbz-Arg-Arg-AMC hydrolysis when compared with the wild-type enzyme. The affects of these mutations on Cbz-Phe-Arg-AMC hydrolysis by OpdB, where phenylalanine is the P₂ residue, were less severe (Table 4), with the D460T-D462N OpdB variant exhibiting only a 28% increase in K_m and a 19% reduction in k_{cat} for Cbz-Phe-Arg-AMC.

DISCUSSION

Salmonella OpdB amidolytic activity was restricted to substrates with basic residues in the P₁ position, while basic, aromatic and hydrophobic residues were accommodated in P₂. While this substrate specificity of was comparable to that of eukaryotic OpdBs, the catalytic power of the enzyme (k_{cat}) was up to fivefold less than that observed for *T. brucei* OpdB (25).

Salmonella OpdB neither demonstrated reductive activation nor was inhibited by thiol-alkylating agents, in contrast to its
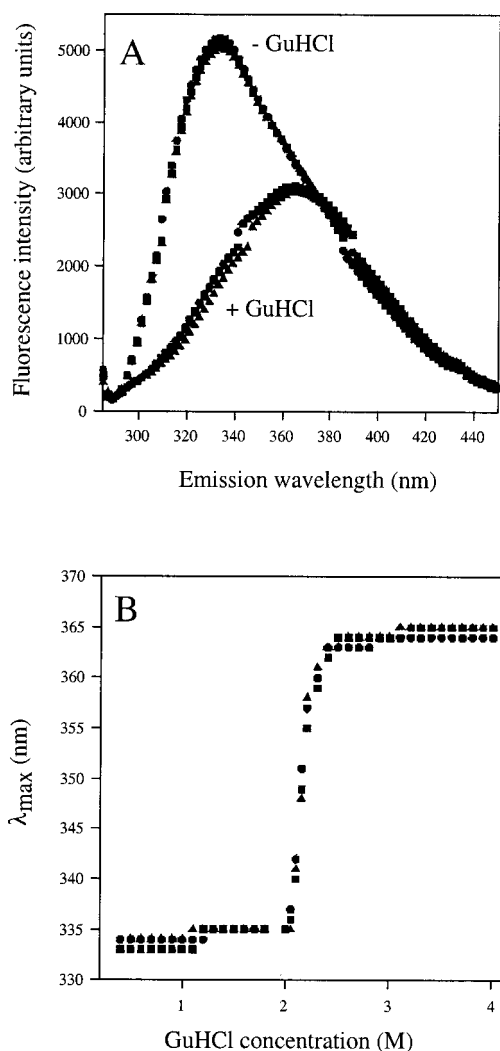
FIG. 4. Equilibrium unfolding transitions by GuHCl. (A) Fluorescence emission spectra for wild-type (●), D460T-D462N (▲), and E576A-E578A (■) OpdB mutant proteins. Each enzyme was 25 μg · ml^{-1} in 50 mM Tris-HCl, pH 8. Spectra were recorded using an excitation wavelength of 278 nm, in the presence (+ GuHCl) and absence (− GuHCl) of 4 M GuHCl. (B) Changes in the λ$_{max}$ of the emission spectra of OpdB wild-type and mutant proteins as a function of denaturant concentration.

eukaryotic relatives (both POP and OpdB) which demonstrate sensitivity to reducing agents, enhancing activity (23, 25), and are potently inhibited by thiol-alkylating agents (7, 25). In porcine POP, this phenomenon is attributed to the reduction or alkylation of a cysteine residue, Cys[255], which is brought into close proximity to the S$_1$ and S$_3$ substrate-binding sites by the folding of the enzyme (7). There is no comparable cysteine residue in the *Salmonella* OpdB sequence we report here, perhaps explaining this observation. Interestingly, a post-proline-cleaving member of the POP family from the prokaryote *Flavobacterium* also does not demonstrate sensitivity to reducing and thiol-alkylating agents either (40). Thus, insensitivity to these agents appears to be a property of members of both branches of the prokaryotic POP family.

TABLE 3. Affect of amino acid substitutions on P$_1$ specificity of OpdB using Cbz-Arg-AMC[a]

Mutant	Kinetics		
	K_m (μM)	k_{cat} (s^{-1})	k_{cat}/K_m (s^{-1} μM^{-1})
Wild type	4.4	9	2
D460T	4.6	10	2
D462N	4.7	10	2
D460T-D462N	5.2	7	1
E494H	4.6	9	2
D567H	5.0	9	2
E576A	33.4	2	0.06
E578A	16.4	4	0.2
E576A-E578A	ND	ND	ND
E576W-E578T	ND	ND	ND
E576R-E578R	ND	ND	ND
D599H	4.5	9	2
E624H	5.4	10	2
D638Q	4.0	11	3

[a] No activity was observed against H-Arg-AMC, H-Leu-AMC, H-Lys-AMC, Cbz-Leu-Leu-Glu-βNA, Cbz-Ala-Ala-Phe-AMC, Cbz-Gly-Gly-Leu-pNA, Suc-Ile-Ala-AMC, Suc-Gly-Pro-AMC, Ac-Tyr-Val-Ala-Asp-pNA, and Suc-Ala-Ala-Pro-Phe-AMC. ND, no detectable activity. The standard errors of the K_m and k_{cat} values were within 10% of their respective means.

Histone proteins were employed as prospective OpdB substrates because they are highly basic proteins (pI > 11) (19) and contain a high proportion of basic residues, thus presenting many potential OpdB cleavage sites. *Salmonella* OpdB degraded human histones H1, H2A, H3, and H4. Cleavage sites in H2A and H4 were located in the N-terminal tail, which projects out from the globular structure of the histone core (19). These tails may thus gain access to the OpdB active site, which by analogy with POP ordinarily excludes proteins with globular tertiary structures via the regulatory β-propeller domain (7). Cleavage was not observed after pairs of basic residues in H2A and H4, possibly because basic amino acid pairs in H2A and H4 are either chemically modified by acetylation or methylation [e.g., Arg[21]Lys(Me)[22] in H4] or locked into

TABLE 4. Affect of amino acid substitutions on P$_2$ specificity of OpdB[a]

Mutant	Amino acid substitution and kinetics					
	Cbz-Arg-Arg-AMC			Cbz-Phe-Arg-AMC		
	K_m (μM)	k_{cat} (s^{-1})	k_{cat}/K_m (s^{-1} μM^{-1})	K_m (μM)	k_{cat} (s^{-1})	k_{cat}/K_m (s^{-1} μM^{-1})
Wild type	0.8	29	36	2.1	21	10
D460T	2.1	22	10	2.9	18	6
D462N	2.3	23	10	3.0	19	6
D460T-D462N	2.9	18	6	2.9	17	6
E494H	1.0	33	33	2.5	18	7
D567H	0.8	29	36	2.0	22	10
E576A	4.5	9	2	12.0	7	0.6
E578A	3.1	9	3	5.9	9	2
D599H	1.0	30	30	2.1	20	10
E624H	1.0	33	33	2.6	22	8
D638Q	1.1	31	28	2.8	20	7

[a] No activity was observed against H-Arg-AMC, H-Leu-AMC, H-Lys-AMC, Cbz-Leu-Leu-Glu-βNA, Cbz-Ala-Ala-Phe-AMC, Suc-Ile-Ala-AMC, Suc-Gly-Pro-AMC, Ac-Tyr-Val-Ala-Asp-pNA, and Suc-Ala-Ala-Pro-Phe-AMC. The standard errors of the values for K_m and k_{cat} were within 10% of their respective means.

α-helices (e.g., Arg[36]Arg[37] in H4) (Fig. 2B) (19). Together, these data suggest that the substrate specificity of OpdB is not as restricted as originally theorized and that proteins, in addition to oligopeptides, are modified by OpdB. However, sites for OpdB hydrolysis in proteins are likely to be confined regions that are not organized into defined, rigid, secondary structures or posttranslationally modified at the P_1 or P_2 residues. These data add to a growing body of evidence that these oligopeptidases hydrolyze protein substrates, albeit in a restricted fashion (for example, the degradation of p40-phox by POP [12]), and lend support to the theory that OpdB is a specialized protein processing enzyme in prokaryotes and lower eukaryotes (30, 32). This theory is also supported by a report of the limited hydrolysis of aspartokinase I-homoserine dehydrogenase by *E. coli* OpdB (28).

To further explore substrate recognition properties of OpdB at a molecular level, we attempted to identify residues that may be determinants of substrate specificity. The POP family of serine peptidases splits into two branches, in terms of substrate specificity (Fig. 1). The archetypical member of this family (POP) hydrolyzes peptide bonds exclusively on the C-terminal side of proline residues in oligopeptides. In contrast, the OpdB branch hydrolyzes peptide bonds exclusively on the C-terminal side of basic residues. An alignment of the catalytic domains of both branches of the POP family (Fig. 3) revealed stretches of sequence that were conserved within respective branches of the phylogenetic tree (Fig. 1) but were consistently different between the two branches. We reasoned that residues contained in these differentially conserved regions were likely to be responsible for substrate specificity, since with the exception of substrate specificity, the physicochemical properties POP and OpdB are similar. Given the specificity of OpdB for cleavage after basic residues, we reasoned that differentially conserved acidic residues were likely determinants of specificity, since they may electrostatically interact with the basic side chains of arginine and lysine residues in substrates. In the present study, we examined the role of nine differentially conserved acidic residues located in the catalytic domain of *Salmonella* OpdB: Asp[460], Asp[462], Glu[494], Asp[567], Glu[576], Glu[578], Asp[599], Glu[624], and Asp[638] (Fig. 3). Mutations in Glu[494], Asp[567], Asp[599], Glu[624], and Asp[638] yielded OpdB variants with substrate hydrolysis profiles similar to those of the wild-type enzyme. We thus concluded that these residues were not determinants of P_1 and P_2 specificity.

Mutations in Glu[576] and Glu[578] significantly altered the hydrolysis of Cbz-Arg-AMC by OpdB, since simultaneous replacement of both Glu[576] and Glu[578] with alanine abolished this activity. Thus, Glu[576] and Glu[578] are critically involved in the interaction of OpdB with the P_1 substrate residue. We propose that the carboxyl groups of Glu[576] and Glu[578] direct OpdB substrate specificity by electrostatic interaction with the charged side chains of P_1 arginine and lysine residues in substrates. This idea is reinforced by the observations that high ionic strength inhibits the hydrolysis of basic substrates by *E. coli* OpdB by elevating the K_m (15, 30), which is most likely attributable to the disruption of electrostatic interactions between substrate arginyl residues and carboxyl groups of the enzyme. Given the close proximity of Glu[576] and Glu[578] to one another (they are separated by a single tryptophan residue in the primary sequence (Fig. 3), we speculate that the side chains

of Glu[576] and Glu[578] form a carboxyl dyad that electrostatically binds the basic side chains of arginine and lysine residues in substrates. In support of this idea, Glu[576] of *Salmonella* OpdB corresponds to Trp[595] of porcine POP, which forms the base of the S_1 specificity pocket of POP and directs P_1 specificity of POP for proline residues, by ring stacking between the tryptophan indole ring and the proline residue (7).

We attempted to change the P_1 specificity of OpdB by mutating Glu[576] and Glu[578] to hydrophobic residues (a E576A-E578A double mutant, thus creating a hydrophobic S_1 pocket) or to basic residues (a E575R-E578R double mutant, thus creating a basic charge environment in the S_1 pocket that could accommodate acidic P_1 side chains). However, both double mutants, which were devoid of activity against the OpdB substrate Cbz-Arg-AMC, also lacked activity against substrates with P_1 hydrophobic residues (bold) (Cbz-Ala-Ala-**Phe**-AMC, Suc-Ile-**Ala**-AMC and Cbz-Gly-Gly-Leu-pNA) and P_1 acidic residues (bold) (Cbz-Leu-Leu-**Glu**-βNA and Ac-Tyr-Val-Ala-**Asp**-pNA). Attempts to convert OpdB specificity to POP specificity by replacing both Glu[576] and Glu[578] with their corresponding residues in POP (Glu[576]→Trp and Glu[578]→Thr) (Fig. 3) yielded an OpdB double mutant (E576W-E578T) that did not exhibit any activity against the OpdB substrate Cbz-Arg-AMC or the POP substrate Suc-Gly-Pro-AMC. Thus, either these variants were misfolded and catalytically incompetent or other residues were involved in directing P_1 specificity. The former possibility seems unlikely, since site-mutated OpdB variants exhibited fluorescence emission spectra identical to that of the wild-type enzyme. More likely, additional residues act in concert with Glu[576] and Glu[578] to define P_1 specificity. Along these lines, differentially conserved sequences (for example, Ser[569] Ile[570] Pro[571] Leu[572] Thr[573] Thr[574]) (Fig. 3) that lack acidic residues are observed in close proximity to Glu[576] and Glu[578] in all OpdB homologues.

Mutations in a second pair of residues, Asp[460] and Asp[462], altered the hydrolytic activity of OpdB against Cbz-Arg-Arg-AMC but had considerably less affect when a hydrophobic residue was in P_2 (phenylalanine, in the case of Cbz-Phe-Arg-AMC). Since these mutations did not affect the hydrolysis of Cbz-Arg-AMC by OpdB, Asp[460] and Asp[462] are not involved in the S_1-P_1 interaction but rather appear to be involved in the recognition of the basic, charged side chain of the P_2 Arg in Cbz-**Arg**-Arg-AMC and thus are involved in directing the specificity of OpdB for cleavage after pairs of basic amino acid residues.

Our kinetic data are nicely supported by the recently published three-dimensional model of OpdB built by Gérczei and coworkers (10). These investigators prepared an homology model of *E. coli* OpdB based on the crystal structure of the closely related porcine prolyl oligopeptidase (7) and docked two substrates, Cbz-Arg-OH and Cbz-Arg-Arg-OH into the OpdB active-site using the Monte Carlo docking method. In this model, the P_2 Arg of Cbz-**Arg**-Arg-OH was bound to the carboxyl groups of Asp[460] and Asp[462], implicating both Asp[460] and Asp[462] in directing P_2 specificity, which we have demonstrated experimentally in this study using site-directed mutagenesis. We thus propose in this study the existence of two carboxyl dyads: one formed by the side chains of Asp[460] and Asp[462], which together direct the OpdB P_2 substrate specificity,

and another formed by the side chains of Glu^{576} and Glu^{578}, which together direct P$_1$ substrate specificity.

ACKNOWLEDGMENTS

REFERENCES

1. Aiyar, A. 2000. The use of CLUSTAL W and CLUSTAL X for multiple sequence alignment. Methods Mol. Biol. 132:221–241.
2. Barrett, A. J., and N. D. Rawlings. 1995. Families and clans of serine peptidases. Arch. Biochem. Biophys. 318:247–250.
3. Barrett, A. J., and N. D. Rawlings. 1992. Oligopeptidases, and the emergence of the prolyl oligopeptidase family. Biol. Chem. Hoppe-Seyler 373:353–360.
4. Burleigh, B. A., E. V. Caler, P. Webster, and N. W. Andrews. 1997. A cytosolic serine endopeptidase from *Trypanosoma cruzi* is required for the generation of Ca^{2+}-signaling in mammalian cells. J. Cell Biol. 136:609–620.
5. Caler, E. V., S. Vaena, P. A. Haynes, N. W. Andrews, and B. A. Burleigh. 1998. Oligopeptidase B-dependent signaling mediates host cell invasion by *Trypanosoma cruzi*. EMBO J. 17:4975–4986.
6. Fenno, J. C., S. Young Lee, C. H. Bayer, and Y. Ning. 2001. The *opdB* locus encodes the trypsin-like peptidase activity of *Treponema denticola*. Infect. Immun. 69:6193–6200.
7. Fülöp, V., Z. Böcskei, and L. Polgár. 1998. Prolyl oligopeptidase: an unusual β-propeller domain regulates proteolysis. Cell 94:161–170.
8. Fülöp, V., Z. Szeltner, and L. Polgár. 2000. Catalysis of serine oligopeptidases is controlled by a gating filter mechanism. EMBO Rep. 1:277–281.
9. Fülöp, V., Z. Szeltner, V. Renner, and L. Polgár. 2001. Structures of prolyl oligopeptidase substrate/inhibitor complexes: use of inhibitor binding for titration of the catalytic histidine residue. J. Biol. Chem. 276:1262–1266.
10. Gérczei, T., G. M. Keserü, and G. Náray-Szabó. 2000. Construction of a 3D model of oligopeptidase B, a potential processing enzyme in prokaryotes. J. Mol. Graph. Model. 18:7–17.
11. Grellier, P., S. Vendeville, R. Joyeau, I. M. Bastos, H. Drobecq, F. Frappier, A. R. Teixeira, J. Schrével, E. Davioud-Charvet, C. Sergheraert, and J. M. Santana. 2001. *Trypanosoma cruzi* prolyl oligopeptidase Tc80 is involved in nonphagocytic mammalian cell invasion by trypomastigotes. J. Biol. Chem. 276:47078–47086.
12. Hasebe, H., J. Hua, A. Someya, P. Morain, F. Checler, and I. Nagaoka. 2001. Involvement of cytosolic prolyl endopeptidase in degradation of p40-phox splice variant protein in myeloid cells. J. Leukoc. Biol. 69:963–968.
13. Heiman, C., and C. G. Miller. 1978. *Salmonella typhimurium* mutants lacking protease II. J. Bacteriol. 135:588–594.
14. Hoiseth, S. K., and B. A. Stocker. 1981. Aromatic-dependent *Salmonella typhimurium* are non-virulent and effective as live vaccines. Nature 291:238–239.
15. Juhász, T., Z. Szeltner, V. Renner, and L. Polgár. 2002. Role of the oxyanion binding site and subsites S1 and S2 in the catalysis of oligopeptidase B, a novel target for antimicrobial chemotherapy. Biochemistry 41:4096–4106.
16. Kahyaoglu, A., K. Haghjoo, F. Guo, F. Jordan, C. Kettner, F. Felföldi, and L. Polgár. 1997. Low barrier hydrogen bond is absent in the catalytic triads in the ground state but is present in a transition state complex in the prolyl oligopeptidase family of serine peptidases. J. Biol. Chem. 272:25547–25554.
17. Kanatani, A., T. Masuda, T. Shimoda, F. Misoka, X. S. Lin, T. Yoshimoto, and D. Tsuru. 1991. Protease II from *Escherichia coli*: sequencing and expression of the enzyme gene and characterization of the expressed enzyme. J. Biochem. 110:315–320.
18. Leite, M. F., M. S. Moyer, and N. W. Andrews. 1998. Expression of the mammalian calcium signaling response to *Trypanosoma cruzi* in *Xenopus laevis* oocytes. Mol. Biochem. Parasitol. 92:1–13.
19. Luger, K., A. W. Mäder, R. K. Richmond, D. F. Sargent, and T. J. Richmond. 1997. Crystal structure of the nucleosome core particle at 2.8 Å resolution. Nature 389:251–260.
20. Maes, M., F. Goossens, S. Scharpé, H. Y. Meltzer, P. D'Hondt, and P. Cosyns. 1994. Lower serum prolyl endopeptidase activity in major depression: further evidence that peptidases play a role in the pathophysiology of depression. Biol. Psychiatry 35:545–552.
21. Matsudaira, P. 1987. Sequence from picomole quantities of proteins electroblotted onto polyvinylene difluoride membranes. J. Biol. Chem. 262:10035–10038.
22. McClelland, M., K. E. Sanderson, J. Spieth, S. W. Clifton, P. Latreille, L. Courtney, S. Porwollik, J. Ali, M. Dante, F. Du, S. Hou, D. Layman, S. Leonard, C. Nguyen, K. Scott, A. Holmes, N. Grewal, E. Mulvaney, E. Ryan, H. Sun, L. Florea, W. Miller, T. Stoneking, M. Nhan, R. Waterton, and R. K. Wilson. 2001. Complete genome sequence of *Salmonella enterica* serovar Typhimurium LT2. Nature 413:852–856.
23. Morty, R. E., E. Authié, L. Troeberg, J. D. Lonsdale-Eccles, and T. H. T. Coetzer. 1999. Purification and characterisation of a trypsin-like serine oligopeptidase from *Trypanosoma congolense*. Mol. Biochem. Parasitol. 102:145–155.
24. Morty, R. E., J. D. Lonsdale-Eccles, R. Mentele, E. A. Auerswald, and T. H. T. Coetzer. 2001. Trypanosome-derived oligopeptidase B is released into the plasma of infected rodents, where it persists and retains full catalytic activity. Infect. Immun. 69:2757–2761.
25. Morty, R. E., J. D. Lonsdale-Eccles, J. Morehead, E. V. Caler, R. Mentele, E. A. Auerswald, T. H. T. Coetzer, N. W. Andrews, and B. A. Burleigh. 1999. Oligopeptidase B from *Trypanosoma brucei*: a new member of an emerging subgroup of serine oligopeptidases. J. Biol. Chem. 274:26149–26156.
26. Morty, R. E., L. Troeberg, R. N. Pike, R. Jones, P. Nickel, J. D. Lonsdale-Eccles, and T. H. T. Coetzer. 1998. A trypanosome oligopeptidase as a target for the trypanocidal agents pentamidine, diminazene and suramin. FEBS Lett. 433:251–256.
27. Morty, R. E., L. Troeberg, J. C. Powers, S. Ono, J. D. Lonsdale-Eccles, and T. H. T. Coetzer. 2000. Characterisation of the antitrypanosomal activity of peptidyl α-aminoalkyl phosphonate diphenyl esters. Biochem. Pharmacol. 60:1497–1506.
28. Pacaud, M., and C. Richaud. 1975. Protease II from *Escherichia coli*. J. Biol. Chem. 250:7771–7779.
29. Polgár, L. 1999. Oligopeptidase B: a new type of serine peptidase with a unique substrate-dependent temperature sensitivity. Biochemistry 38:15548–15555.
30. Polgár, L. 1997. A potential processing enzyme in prokaryotes: oligopeptidase B, a new type of serine peptidase. Proteins 28:375–379.
31. Polgár, L. 1994. Prolyl oligopeptidases. Methods Enzymol. 244:188–200.
32. Polgár, L., and F. Felföldi. 1998. Oligopeptidase B: cloning and probing stability under nonequilibrium conditions. Proteins 30:424–434.
33. Salvesen, G., and H. Nagase. 1989. Inhibition of proteolytic enzymes, p. 83–104. *In* R. J. Benyon and J. S. Bond (ed.), Proteolytic enzymes: a practical approach. IRL Press, Oxford, United Kingdom.
34. Schägger, H., and G. von Jagow. 1987. Tricine-sodium dodecyl sulfate-polyacrylamide gel electrophoresis for the separation of proteins in the range from 1 to 100 kDa. Anal. Biochem. 166:368–379.
35. Schechter, I., and A. Berger. 1967. On the size of the active-site in proteases. I. Papain. Biochem. Biophys. Res. Commun. 32:898–902.
36. Toide, K., M. Shinoda, and A. Miyazaki. 1998. A novel prolyl endopeptidase inhibitor, JTP-4819—its behavioural and neurochemical properties for the treatment of Alzheimer's disease. Rev. Neurosci. 9:17–29.
37. Troeberg, L., R. N. Pike, R. E. Morty, R. K. Berry, T. H. T. Coetzer, and J. D. Lonsdale-Eccles. 1996. Proteinases from *Trypanosoma brucei brucei*: purification, characterisation and interactions with host regulatory molecules. Eur. J. Biochem. 238:728–734.
38. Wilson, K. 1987. Preparation of genomic DNA from bacteria, p. 2.4.1–2.4.5. *In* F. M. Ausubel, R. Brent, R. E. Kingston, D. D. Moore, J. G. Seidman, J. A. Smith, and K. Struhl (ed.), Current protocols in molecular biology, vol. 1. John Wiley & Sons, New York, N.Y.
39. Yoshimoto, T., K. Kado, F. Matsubara, N. Koriyama, H. Kaneto, and D. Tsuru. 1987. Specific inhibitors for prolyl oligopeptidase and their anti-amnesic effect. J. Pharmacobiodyn. 10:730–735.
40. Yoshimoto, T., A. Kanatani, T. Shimoda, T. Inaoka, T. Kokubo, and D. Tsuru. 1991. Prolyl endopeptidase from *Flavobacterium meningosepticum*: cloning and sequencing of the enzyme gene. J. Biochem. 110:873–878.
41. Yoshimoto, T., J. Tabira, T. Kabashima, S. Inoue, and K. Ito. 1995. Protease II from *Moraxella lacunata*: cloning, sequencing, and expression of the enzyme gene, and crystallization of the expressed enzyme. J. Biochem. 117:654–660.